Scientific Research Publishing

New Journal of Glass and Ceramics, 2021, 11, 34-43
https://www.scirp.org/journal/njgc
ISSN Online: 2161-7562
ISSN Print: 2161-7554

Structural Role of CeO_2 in the Modified Borate Glass-Ceramics

Nada ElBaz[1], Gomaa El-Damrawi[1*], Amr M. Abdelghany[2]

[1]Glass Research Group, Faculty of Science, Physics Department, Mansoura University, Mansoura, Egypt
[2]Spectroscopy Department, Physics Division, National Research Centre, Giza, Egypt
Email: *gomaaeldamrawi@gmail.com

How to cite this paper: ElBaz, N., El-Damrawi, G. and Abdelghany, A.M. (2021) Structural Role of CeO_2 in the Modified Borate Glass-Ceramics. *New Journal of Glass and Ceramics*, **11**, 34-43.
https://doi.org/10.4236/njgc.2021.111002

Received: December 17, 2020
Accepted: January 24, 2021
Published: January 27, 2021

Abstract

A new type of cerium borate glass-ceramic is prepared and studied. The microstructure and crystallization behaviors of the glass samples were investigated by X-ray diffraction (XRD), electron diffraction (ED), and ^{31}P NMR spectroscopy. The microstructures of samples contain <1 mol% CeO_2 are amorphous in nature. More addition of CeO_2 transforms the glass to glass-ceramics without thermal annealing. The morphological change of the microstructure of these materials was followed by transmission electron microscopy (TEM). The obtained results have revealed that the addition of more than 0.8 mol% CeO_2 can promote nucleation and crystallization routes that are combined with the establishment of diverse crystalline phases. Glasses with lower contents of CeO_2 showed no tendency to crystallization. The crystals of CeO_2 containing glasses were spheroid like morphology that was assigned to the three-dimensional fast growth of the well-formed structural species in the boro-apatite phase. In addition, the cerium free glass is characterized by particle-like morphology. Then the growth of spheroid species in three-dimension plays better compatibility and bioactivity behavior than that of the other types of morphology. This is may because the spherical shape has a higher surface area than that of the needle-like morphology. Accumulation and aggregation of small-sized spheres from cerium borate phases played the role of enhancing the hardness of the studied materials.

Keywords

Cerium Borate, Glass Morphology, Crystalline State, Spheroid Species

1. Introduction

It has been reported previously that the hydrated calcium phosphate structure known as hydroxyapatite (HA) is considered to be biocompatible with human

hard tissues and displays Osseo conductive characteristics [1] [2]. Accordingly, HA can be assumed as superior material for clinical and medical applications. However, HA is well known to have reduced mechanical strength in comparison with natural bone. This drawback is assumed to be the most serious obstacle for some specific claims, particularly for load-bearing implants [3] [4]. For this reason, bioactive glass-ceramics are considered as alternatives to the pure HA to be used as fillers and bone graft [5]. This may due to their enhanced hardness and mechanical strength which lead to their good ability to form strong bonds with living bone [6]. Besides, the apatite of such bioglass-ceramics has to be characterized by its good crystalline structure. The enhanced crystallinity leads to mechanical strength and biocompatibility stronger than that of the pure HA. Consequently, load bearing applications appear to need a perfect mix of bioactivity and preferred mechanical characteristics of crystalline apatite phases to be used.

Recently, developing new biomaterials was focused on silica free glasses and glass-ceramics [7] [8] [9] resulting from the ease crystallization of the apatite phases through stimulating suitable environments including doping with activating agents such as CeO_2, Nd_2O_3, CrF_2, etc. [10] [11] [12]. Besides, the precipitation of crystalline apatite phases within the as-prepared glass network was expected to be enhanced [10]. It was reported that amorphous glasses were considered to have a limited bioactivity in comparison to that of natural bones. But the crystallized glass-ceramics can simply possess the biocompatibility and tight bonding to the bone subsequent in the growth of healthy tissues to their surfaces [11].

Mechanical properties were observed to be enhanced using different amalgamations among apatite and various glass phases. Amongst them, apatite $Ca_5(PO_4)_3$, wollastonite ($CaSiO_3$) or $CaTeO_3$ have been suggested to be used as clinically bone-repairing materials [13] [14] [15]. Besides, flour—apatite ($Ca_5(PO_4)_3$ F—is conveyed as a customary type which is can be considered as a promising material in biodental applications including dental roots, and joint prostheses.

Recent researches have been focused on silicate free glasses as bioactive materials. Studies on borate and mixed former borophosphates, to our knowledge, are growing field of studies reported by several authors [7] [8] [9]. Therefore, trials will be done in this work to explore the bioactive properties and structure of borate glass-ceramics as a new biomaterial. Moreover, borate glasses containing CeO_2 (as an agent for crystallization) will be studied. The presence of CeO_2 in the network of borate network will enhance the bioactivity of the material since CeO_2 is reported to be used as a nucleating and crystallizing agent of apatite and wollastonite phases.

2. Experimental Methods

Glasses of basic composition $x CeO_2 \cdot (45 - x) B_2O_3 \cdot 24.5 Na_2O \cdot 24.5 CaO \cdot 6 P_2O_5$ were synthesized using ordinary melt annealing technique. Pure analytical grade chemical of ceric oxide supplied by Sigma Aldrich Co., orthoboric acid, ammo-

nium dihydrogen phosphate, sodium and calcium were used in their carbonate form supplied by ElNasr pharmaceuticals. Glass nomination and composition was listed in Table 1.

X-ray diffractogram of the studied samples is recorded using PAN analytical X-Pert PRO machine operated with 30 kV utilizing copper target with $\lambda_{k\alpha}$ = 1.540 Å within Braggs angles extended from 4˚ to 70˚. Surface and bulky morphologies of studied samples were recorded using (JEOL, JSM-5400) scanning and transmission electron microscopy (SEM. TEM) supported with EDAX and ED units, respectively. Studied samples were coated with a thin layer of gold. The Vickers microhardness numbers (HV) was recorded as an average of 15 indentation in a triplicate sample measured in a polished surface using FM-7 micro hardness tester at 25-g force load to ensure homogeneity and reproducibility of measurements.

^{31}P MAS NMR experiments were also conducted at resonance frequency (202.4 MHz) using a 3.2 mm diameter rotor spinning at 15 kHz. Solid $NH_4H_2PO_4$ was used as a secondary reference compound and the signal from this set to 0.8 ppm. A pulse length of 2.5 μs and a recycle delay of 5 s was applied.

3. Results Discussion

Figure 1 and Figure 2 show the XRD spectra of the studied glasses as a function of CeO_2 concentration. The XRD spectra of glasses which contain low CeO_2 concentration (0, 0.5 and 0.8) Figure 1 possess a wide hump that supports the amorphous structure of these glasses. On the other hand, glasses of higher CeO_2 concentrations (Figure 2) exhibit intense sharp diffraction peaks superimposed on a widespread diffraction hump. The sharpness of several peaks may is due to the presence of different phases enriched with fine crystals in the investigated samples.

Positions of indicated sharp diffraction peaks on XRD diffractogram shown in Figure 2 is compatible with that reported for cerium sodium borate and calcium

Table 1. Glass abbreviation and composition.

Abbr.	CeO_2	B_2O_3	Na_2O	CaO	P_2O_5
Ce0	0.00	45.0	24.5	24.5	6.0
Ce0.5	0.50	44.5	24.5	24.5	6.0
Ce0.8	0.80	44.2	24.5	24.5	6.0
Ce1	1.00	44.0	24.5	24.5	6.0
Ce2	2.00	43.0	24.5	24.5	6.0
Ce4	4.00	41.0	24.5	24.5	6.0
Ce8	8.00	37.0	24.5	24.5	6.0
Ce12	12.0	33.0	24.5	24.5	6.0
Ce20	20.0	25.0	24.5	24.5	6.0

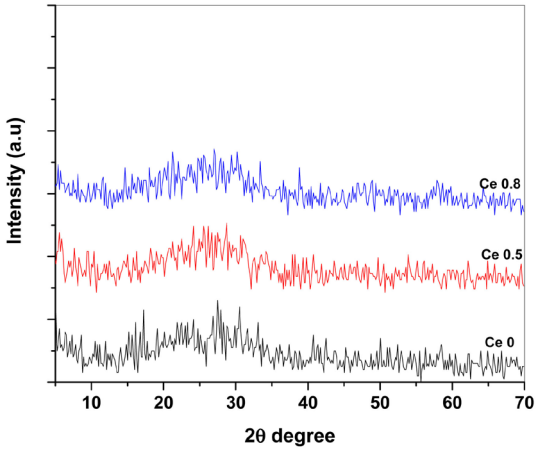

Figure 1. XRD spectra of glasses containing 0, 0.5 and 0.8 mol% CeO_2.

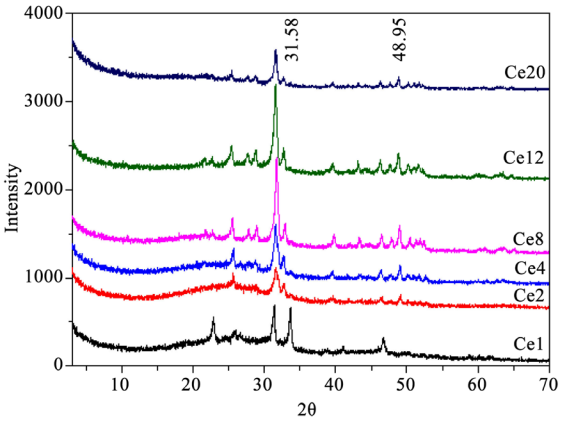

Figure 2. X-ray diffraction (XRD) patterns of borate glasses containing different CeO_2 concentrations.

phosphate phases [16]. These phases were classified as $Ca_2CeB_2O_7$ and $Na_4CeB_2O_7$, in combination with various calcium phosphate phases as, $Ca_2(P_2O_7)$ and $CaCe(PO_3)$. These phases were considered to be amongst the most bioactive and biocompatible phases in the matrix of the borophosphate glass-ceramics network [17].

The crystalline phases presented by CeO_2 rich borate glasses can precipitate apatite units with Ca/P ratio near to unity [18] [19]. This leads that adequate degree of crystallinity is enhanced by the effect of more CeO_2 addition as can be seen from **Figure 3**.

Results based on TEM and EDP, (**Figure 4**) agree well with that obtained from XRD. Both would confirm the amorphous nature of glasses containing low concentrations of CeO_2. **Figure 4(a)** is introduced as an example (0.8 mol% CeO_2). There are no resolved electron diffraction patterns due to the amorphous nature of glassy samples while no ordered structure can be detected. Then it can be concluded that the ceramics with $CeO_2 < 1$ mol% show a common microstructure that contains nonuniform distributed species. On the other hand, TEM micrographs of samples contain higher CeO_2 concentration indicates that spheroids

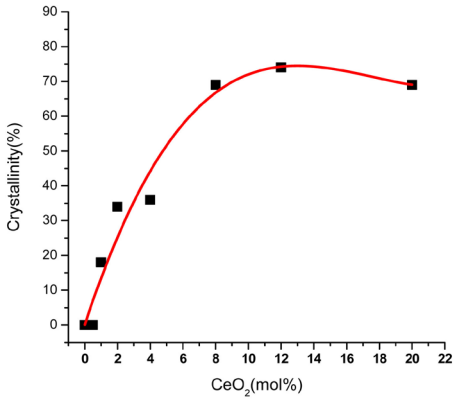

Figure 3. Crystallinity changes as a function of cerium content.

morphology as the most dominant morphology. Such spheroid crystals can be observed to cover utmost of the studied area of the sample under investigation. The growing of spherical crystals (**Figures 4(b)-(d)**) is the main feature of the cerium ions which can be distributed in any glass composition. Simply, on increasing CeO_2 contents the microstructure is appeared to contain clearer distributed species with less grain boundaries and less porosities (**Figure 4(b)**). However, larger amounts of CeO_2 result in the complexation of microstructure. For the ceramics with CeO_2 = 8, 15 and 20 mol%, the microstructure becomes crowded with some anisometric layers containing some polycrystalline species. The existence of these interconnected layers, can enhance the mechanical strength, since the hardness-number **Figure 5** is found to increase with increasing CeO_2 concentrations. This is attributed to the increase of CeO_4 concentration which leads to enhancing the phase formation caused by higher content of CeO_4. The presence of the polycrystalline phases enriched with CeO_4 enhances the hardness number of the glass and decreases the crack length due to indentation processes (**Figure 5**) and reduces the grain growth.

It can be shown from TEM micrographs that the capacity of precipitated crystal increases with increasing CeO_2 concentration. For instance, accumulation of the precipitated crystals is increased and distributed in multilayers which causes a darkness of the bulk structure of the investigated sample. The high capacity of the crystalline species results in the interconnections between the spheres distributed in several layers. The EDP of cerium rich phase, **Figure 4**, clearly reveals the sharpest diffraction rings confirmed the highest crystallinity of composition contains 20 mol%.

The surface morphology of two selected samples is represented by scanning electron micrographs (SEM) **Figure 6**. It can be shown that there is a great difference between the morphologies presented for sample of low CeO_2 (0.8 mol%) and of the highest CeO_2 concentration (20 mol%). The scanned surface of sample of 20 mol% CeO_2 contains a crystalline species of larger size than that presented for sample of 0.8 mol% CeO_2. The capacity of the accumulated phases is considered as the main reason for appearance of EDS peak with higher intensity than that of 0.8 glass. In addition, EDEX spectra a composition of 20 mol%

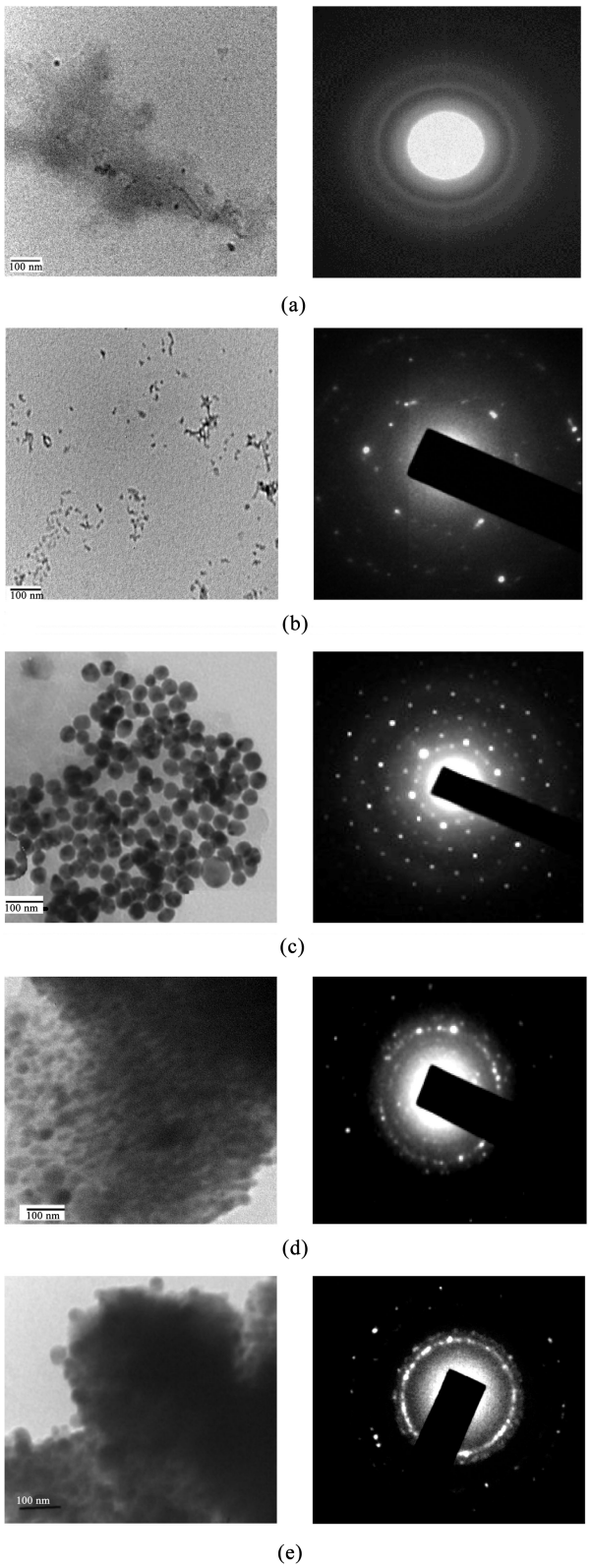

Figure 4. Transmission electron micrographs supported with electron diffraction (TEM/ED) of some selected samples containing variable amounts of cerium oxide. (a) 0.8 mol% CeO_2; (b) 2.0 mol% CeO_2; (c) 8.0 mol% CeO_2; (d) 15 mol% CeO_2; (e) 20 mol% CeO_2.

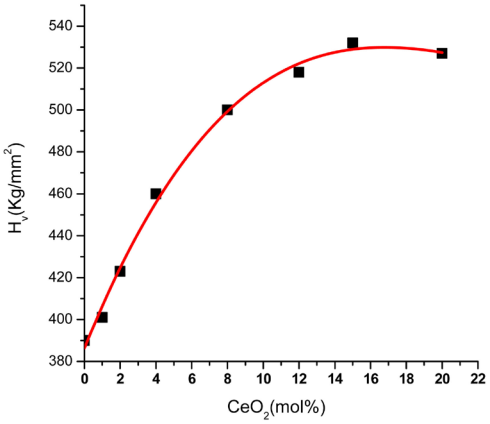

Figure 5. Vicker's hardness (H_V) number as a function of cerium content.

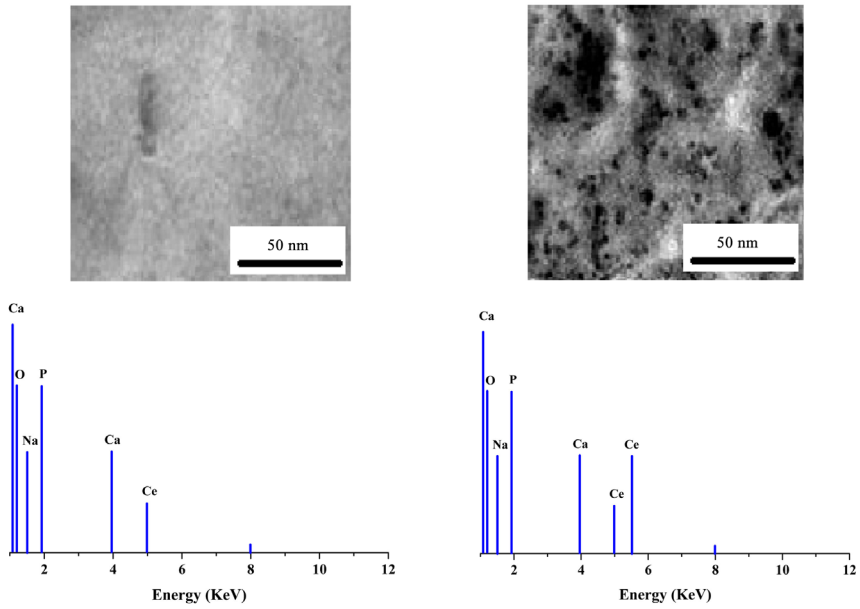

Figure 6. SEM/EDAX micrographs of selected samples containing 0.8 and 20 mol% CeO_2.

CeO_2 contains duple peak for Ce^{2+} ions which confirm more accumulation of crystalline borate species involving Ce ions.

^{31}P MAS NMR experiments offer direct information about the Q^n units in the phosphate network of the investigated glasses. (Q) is P ions and (n) is the number of bridging bonds. The Q^0 species have been found in the main glass network. It is shown in **Figure 7** that the chemical shift value of glasses containing 0 and 2 mol% CeO_2 is in the order of Q0 species (9 ppm) which is the dominant structural species. The frequency peaks of glasses of 0 and 2 mol% CeO_2 compositions are considered to corresponding to orthophosphate Na_3PO_4 or $Ca_3(PO_4)_2$ or mixing between them. Adding of more CeO_2 has some effect on the ^{31}P-NMR spectra, since the value of chemical shift is relatively changed in composition of 12 and 20 mol% CeO_2 glasses (around 2 ppm for composition 20 mol% CeO_2), **Figure 7**. These changes may be considered due to a mixture of cerium sodium

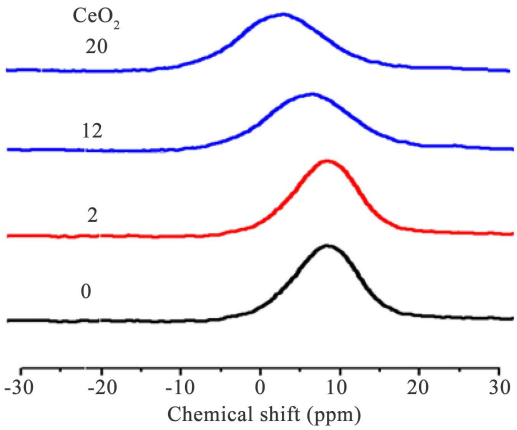

Figure 7. ^{31}P NMR spectra of borate glass Ce free and of glasses containing different CeO_2 concentrations.

or calcium phosphate crystalline phases. The decrease of chemical shift from 9 to 2 ppm means that some of cerium cations are coordinated with PO_4 groups forming cerium phosphate phases [20] [21].

There is a second remark on ^{31}P NMR spectra of glass containing 12 and 20 mol CeO_2. The spectra are relatively broader than that of glasses containing 0 and 2 mol%. This may be considered due to formation of some ordered apatite phases containing Ce ions as a charge compensator, since Ce-O-P bond is longer than that of P-ONa^+.

4. Conclusion

From all above spectra, it can be concluded that the small change in NMR chemical shift of phosphate network (9 to 2 ppm) upon CeO_2 addition should be due to some modification of phosphate network by CeO_2. This means that few of CeO_2 are consumed to modify the phosphate network. But most of CeO_2 concentrations are highly consumed to modify B_2O_3 network resulting in creation high reduction in the fraction of boron tetrahedral units.

Conflicts of Interest

The authors declare no conflicts of interest regarding the publication of this paper.

References

[1] Ning, C.Q. and Zhou, Y. (2002) *In Vitro* Bioactivity of a Biocomposite Fabricated from HA and Ti Powders by Powder Metallurgy Method. *Biomaterials*, **23**, 2909-2915. https://doi.org/10.1016/S0142-9612(01)00419-7

[2] Wu, Y., Hench, L.L., Du, J., Choy, K.L. and Guo, J. (2004) Preparation of Hydroxyapatite Fibers by Electrospinning Technique. *Journal of the American Ceramic Society*, **87**, 1988-1991. https://doi.org/10.1111/j.1151-2916.2004.tb06351.x

[3] Gautier, S., Champion, E., Bernache-Assollant, D. and Chartier, T. (1999) Rheological Characteristics of Alumina Platelet-Hydroxyapatite Composite Suspensions. *Journal of the European Ceramic Society*, **19**, 469-477.

https://doi.org/10.1016/S0955-2219(98)00224-6

[4] Cao, W. and Hench, L.L. (1996) Bioactive Materials. *Ceramics International*, **22**, 493-507. https://doi.org/10.1016/0272-8842(95)00126-3

[5] Boccaccini, A.R., Erol, M., Stark, W.J., Mohn, D., Hong, Z. and Mano, J.F. (2010) Polymer/Bioactive Glass Nanocomposites for Biomedical Applications: A Review. *Composites Science and Technology*, **70**, 1764-1776. https://doi.org/10.1016/j.compscitech.2010.06.002

[6] Arcos, D. and Vallet-Regí, M. (2010) Sol-Gel Silica-Based Biomaterials and Bone Tissue Regeneration. *Acta Biomaterialia*, **6**, 2874-2888. https://doi.org/10.1016/j.actbio.2010.02.012

[7] Rahaman, M.N., Day, D.E., Bal, B.S., Fu, Q., Jung, S.B., Bonewald, L.F. and Tomsia, A.P. (2011) Bioactive Glass in Tissue Engineering. *Acta Biomaterialia*, **7**, 2355-2373. https://doi.org/10.1016/j.actbio.2011.03.016

[8] Hoppe, A., Güldal, N.S. and Boccaccini, A.R. (2011) A Review of the Biological Response to Ionic Dissolution Products from Bioactive Glasses and Glass-Ceramics. *Biomaterials*, **32**, 2757-2774. https://doi.org/10.1016/j.biomaterials.2011.01.004

[9] ElBatal, H.A., El-Kheshen, A.A., Ghoneim, N.A., Marzouk, M.A., ElBatal, F.H., Fayad, A.M., El-Beih, A.A., *et al.* (2019) *In Vitro* Bioactivity Behavior of Some Borophosphate Glasses Containing Dopant of ZnO, CuO or SrO Together with Their Glass-Ceramic Derivatives and Their Antimicrobial Activity. *Silicon*, **11**, 197-208. https://doi.org/10.1007/s12633-018-9845-9

[10] Kaur, P., Singh, K.J., Yadav, A.K., Kaur, S., Kaur, R. and Kaur, S. (2020) Growth of Bone like Hydroxyapatite and Cell Viability Studies on CeO_2 Doped CaO-P_2O_5-MgO-SiO_2 Bioceramics. *Materials Chemistry and Physics*, **243**, Article ID: 122352. https://doi.org/10.1016/j.matchemphys.2019.122352

[11] Eslami, M., Hamnabard, Z. and Nemati, A. (2013) Synthesis and Spectral Properties of Nd-Doped Glass-Ceramics in SiO_2-CaO-MgO System Prepared by Sol-Gel Method. *Journal of Rare Earths*, **31**, 595-599. https://doi.org/10.1016/S1002-0721(12)60326-3

[12] El-Damrawi, G., Abou Elzahab, M., Dowadair, A. and Hosny, A. (2019) Electron Paramagnetic Resonance Study on Phosphosilicate Glasses. *Magnetic Resonance in Solids*, *Electronic Journal*, **21**, 19102. https://doi.org/10.26907/mrsej-19102

[13] Vogel, W. and Höland, W. (1987) The Development of Bioglass Ceramics for Medical Applications. *Angewandte Chemie International Edition in English*, **26**, 527-544. https://doi.org/10.1002/anie.198705271

[14] Verne, E., Ferraris, M. and Jana, C. (1999) Pressureless Sintering of Bioverit® III/Ti Particle Biocomposites. *Journal of the European Ceramic Society*, **19**, 2039-2047. https://doi.org/10.1016/S0955-2219(99)00036-9

[15] Kokubo, T. (1998) Apatite Formation on Surfaces of Ceramics, Metals and Polymers in Body Environment. *Acta Materialia*, **46**, 2519-2527. https://doi.org/10.1016/S1359-6454(98)80036-0

[16] Menazea, A.A. and Abdelghany, A.M. (2020) Gamma Irradiated Hench's Bioglass and Their Derivatives Hench's Bioglass-Ceramic for Bone Bonding Efficiency. *Radiation Physics and Chemistry*, **174**, Article ID: 108932. https://doi.org/10.1016/j.radphyschem.2020.108932

[17] Chen, R.S., Huang, J.G., Lu, L. and Xu, Y. (1988) Study of the New Boron-Rich Calcium Rare Earth Borate $CaLnB_7O_{13}$. *Materials Research Bulletin*, **23**, 1699-1704. https://doi.org/10.1016/0025-5408(88)90178-X

[18] Ouis, M.A., Abdelghany, A.M. and ElBatal, H.A. (2012) Corrosion Mechanism and Bioactivity of Borate Glasses Analogue to Hench's Bioglass. *Processing and Application of Ceramics*, **6**, 141-149. https://doi.org/10.2298/PAC1203141O

[19] Abdelghany, A.M., Meikhail, M.S., Hegazy, E., Badr, S.I. and Agag, D.A. (2019) Synthesis of Borate Modified Bioactive Glass Scaffold Using PVP Burning-Out Method for Bone Tissue Replacement. *Biointerface Research in Applied Chemistry*, **9**, 4044-4049. https://doi.org/10.33263/BRIAC94.044049

[20] Atkinson, I., Anghel, E.M., Petrescu, S., Seciu, A.M., Stefan, L.M., Mocioiu, O.C., Zaharescu, M., *et al.* (2019) Cerium-Containing Mesoporous Bioactive Glasses: Material Characterization, *In Vitro* Bioactivity, Biocompatibility and Cytotoxicity Evaluation. *Microporous and Mesoporous Materials*, **276**, 76-88. https://doi.org/10.1016/j.micromeso.2018.09.029

[21] Varini, E., Sánchez-Salcedo, S., Malavasi, G., Lusvardi, G., Vallet-Regí, M. and Salinas, A.J. (2019) Cerium (III) and (IV) Containing Mesoporous Glasses/Alginate Beads for Bone Regeneration: Bioactivity, Biocompatibility and Reactive Oxygen Species Activity. *Materials Science and Engineering: C*, **105**, Article ID: 109971. https://doi.org/10.1016/j.msec.2019.109971